

perature factor (B) of 3.5 \AA^2 . Anomalous dispersion terms were applied to the scattering of Ni. The molecule is diastereomeric, and only one isomer is present in the crystal. Least-squares refinement converged to $R = 0.050$ and $R_w = 0.067$. The maximum and minimum peaks on a final difference electron density map were 0.4 e\AA^{-3} . Final positional and thermal parameters are listed in Tables S.3 and S.4 as supplementary material.

X-ray Crystallographic Analysis of 9b. A deep purple crystal suitable for an X-ray crystallographic study was grown from a methylene chloride solution and mounted on a glass fiber. Data were collected to a maximum $2\theta = 50^\circ$ at 298 K. The position of the Cu atom was obtained from the Patterson synthesis. All remaining atoms, including hydrogen atoms, were located in subsequent difference Fourier maps. The Cu atom and non-hydrogen atoms of the pyrazole fragment were refined anisotropically, and the remaining non-hydrogen atoms were refined isotropically. The positions of all hydrogens were located, refined, and assigned an arbitrary temperature factor (B) of 3.0 \AA^2 . Anomalous dispersion terms were applied to the scattering of Cu. The molecule is diastereomeric, and only one isomer is present in the crystal. Least-squares refinement converged to $R = 0.055$ and $R_w = 0.071$. The maximum and minimum peaks on a final difference electron density map were 0.8 e\AA^{-3} . Final positional and thermal parameters are listed in Tables S.3 and S.4 as supplementary material.

X-ray Crystallographic Analysis of 10b. A deep red crystal suitable for an X-ray crystallographic study was grown from a methylene chloride solution and mounted on a glass fiber. Data were collected to a maximum $2\theta = 50^\circ$ at 298 K. The Fe atom and all the other non-hydrogen atoms were refined anisotropically. The positions of all hydrogens were located and assigned u values of 0.05 \AA^2 . Anomalous dispersion terms were applied to the scattering of Fe. Both isomers of the racemate are present in the crystal. Least-squares refinement converged to $R = 0.034$ and $R_w = 0.049$. The maximum and minimum peaks on a final difference electron density map were 0.3 e\AA^{-3} . Final positional and thermal parameters are listed in Tables S.3 and S.4 as supplementary material.

X-ray Crystallographic Analysis of 11b-2C₆H₅CH₃. An orange crystal suitable for an X-ray crystallographic study was grown from an ethyl acetate/toluene solution and mounted on a glass fiber. Data were collected to a maximum $2\theta = 50^\circ$ at 298 K. The Co atom, two oxygen atoms of the carboxylic acid fragment, and the C atoms of a toluene solvate were refined anisotropically, and all other atoms were refined isotropically. One of the toluene molecules exhibited disorder about a center of symmetry. Methyl hydrogens for the ordered toluene molecule were included in calculated positions as members of a rigid group: C-H = 1.0 \AA , H-C-H = 109.5° , $u = 0.15 \text{ \AA}^2$. No hydrogen atoms were included for the disordered toluene molecule. All phenyl rings were included as rigid, kept in located positions, $u = 0.089 \text{ \AA}^2$. Anomalous dispersion terms were applied to the scattering of Co. The molecule is diastereomeric, and only one isomer is present in the crystal. Least-squares refinement converged to $R = 0.082$ and $R_w = 0.096$. The maximum and minimum peaks on a final difference electron density map were 0.23 e\AA^{-3} . Final positional and thermal parameters are listed in Tables S.3 and S.4 as supplementary material.

Acknowledgment. We thank the National Institutes of Health for support of this research under Grants RO1-CA 31753 and PO1-CA 43904. S.E.J. gratefully acknowledges the National Science Foundation for support from a NSF postdoctoral fellowship (CHE90-01819). F.A.G. gratefully acknowledges the NIH for support from a MARC NIH predoctoral fellowship (GM11586).

Supplementary Material Available: Tables of bond distances and angles, positional and equivalent isotropic thermal parameters, and anisotropic thermal parameters, and details of the crystallographic data collection (51 pages); tables of observed and calculated structure factors (72 pages). Ordering information is given on any current masthead page.

Mechanisms of Cage Reactions: Kinetics of Combination and Diffusion after Picosecond Photolysis of Iron(II) Porphyrin Ligated Systems

Teddy G. Traylor,* Douglas Magde,* Jikun Luo, Kevin N. Walda, Debkumar Bandyopadhyay, Guo-Zhang Wu, and Vijay S. Sharma

Contribution from the Department of Chemistry, University of California, San Diego, 9500 Gilman Drive, La Jolla, California 92093-0506. Received November 22, 1991.

Revised Manuscript Received June 29, 1992

Abstract: The kinetics of transient absorption changes for a number of protoheme-ligand systems after subpicosecond photolysis have been investigated. When the photolyzed ligand is *tert*-butyl, pentachlorophenyl, pentafluorophenyl, 5α -cholestan- 3α -yl, or 5α -cholestan- 3β -yl isocyanide or 1-methylimidazole, a concentration-independent relaxation is observed. Its decay is accurately exponential. Therefore the geminate pair created by photolysis disappears in a clear first-order process and does not follow the power law kinetics reported for similar systems with other ligands in high-viscosity solvents or in glasses at low temperatures. Proteins combining with isocyanides also show exponential geminate recombination with a rate constant of $\sim 10^{11} \text{ s}^{-1}$, which is very close to that of the model systems. Geminate return of carbon monoxide to 1-methylimidazole-protoheme in glycerol is much slower ($3 \times 10^9 \text{ s}^{-1}$) but is also almost exponential.

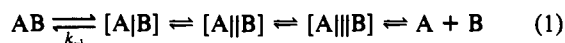
Introduction

Reactions in which combination of reaction partners is competitive with diffusive separation have been treated with two distinct mechanistic theories¹⁻⁸ which emphasize either the sta-

tistical diffusion of the two nonattractive partners through the solvent or activation-controlled passage through a series of distinct (e.g. solvation) states of different energies. In either case, we might represent the process as shown in eq 1, where the vertical lines

- (1) Smoluchowski, M. V. *Z. Phys. Chem.* **1917**, *92*, 129.
- (2) Noyes, R. M. *Prog. React. Kinet.* **1961**, *1*, 129.
- (3) (a) Collins, F. C.; Kimball, G. E. *J. Colloid Sci.* **1949**, *4*, 425. (b) Olea, A. F.; Thomas, J. K. *J. Am. Chem. Soc.* **1988**, *110*, 4494.
- (4) Frauenfelder, H.; Wolynes, P. G. *Science* **1985**, *229*, 337.
- (5) (a) Karim, O. A.; McCammon, J. A. *J. Am. Chem. Soc.* **1986**, *108*, 1762. (b) Ciccotti, G.; Ferrario, M.; Hynes, J. T.; Kapral, R. *J. Chem. Phys.* **1990**, *93*, 7137.
- (6) Alwattar, A. H.; Lumb, M. D.; Birks, J. B. In *Organic Molecular Photophysics*; Birks, J. B., Ed.; Wiley: New York, 1973; Vol. 1, 403.

- (7) Rice, S. A. In *Comprehensive Chemical Kinetics*; Bamford, C. H., Compton, R. G., Eds.; Elsevier: New York, 1985; Vol. 25.
- (8) (a) Winstein, S.; Clippinger, E.; Fainberg, A. H.; Robinson, G. C. *J. Am. Chem. Soc.* **1954**, *76*, 2597. (b) Winstein, S.; Klinedinst, P. E., Jr.; Robinson, G. C. *J. Am. Chem. Soc.* **1961**, *83*, 885. (c) Winstein, S.; Klinedinst, P. E., Jr.; Clippinger, E. *J. Am. Chem. Soc.* **1961**, *83*, 4986. (d) Winstein, S.; Robinson, G. C. *J. Am. Chem. Soc.* **1958**, *80*, 169 and related papers. For reviews see: (e) Harris, J. M. *Prog. Phys. Org. Chem.* **1974**, *11*, 89. (f) Szwarc, M., Ed. *Ions and Ion Pairs in Organic Reactions*; Wiley-Interscience: New York, 1974; Vol. 2, Chapter 3, p 247 ff.



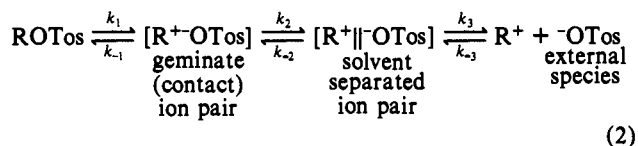
imply greater distances between A and B and perhaps changes in solvation.

The statistical treatment of Smoluchowski¹ assumes that A and B are hard spheres diffusing through a resistive medium and that the diffusional and bond-making processes are separate. The result of this treatment is that the covalent state, AB, is formed by return from A + B pairs of various separation distances. The consequence is a complex nonexponential process extending over long time periods after the AB bond is broken thermally or by a light pulse. We will refer to this as diffusive recombination. Whatever the detailed behavior of the geminate partners may be in a particular case at short times, their recombination behavior must asymptotically become "Smoluchowski-like" at longer times. However, there is no assurance that the range of times for the conditions needed to produce diffusive recombination will correspond to amounts of recombination large enough to measure. Extensive recombination may take place at early times before the approximations built into presently available calculations for diffusive recombination are satisfied; and at long times, the diffusive geminate recombination, which must exist, may well be too small to measure or be swamped by bimolecular combination with the reservoir of (nongeminate) reaction partners.

The alternative approach invokes discrete species AB, [AB], and [A||B], which differ not only in the AB distance but in the type and energy of solvation. In the extreme limit for this model, the energy minima for these species are separated by barriers which involve bond strength, ion-ion, ion-dipole, or dipole-dipole interactions of A with B and specific solvation of the different species. This theory necessarily leads to first-order reactions converting one species to the next.⁹ We will refer to this as kinetic recombination. The kinetic model is mathematically very simple and is expected to dominate the kinetics in those cases where intermediate species are separated by sufficiently large energy barriers. There is still some question as to whether these large energy barriers are present in geminate pairs.

In the majority of cases, one might expect either that the kinetic model might apply at early times and the diffusive model at later times or that a more complicated model intermediate between the extremes would be better. However, detailed intermediate theories have not been proposed yet, presumably because of the paucity of accurate experimental data available to challenge even the simplified extreme theories.

Three different kinds of reactions have been studied in the context of these theories. The first category involves ionic partners. Winstein et al.⁸ showed that stereochemistry and salt effects in the solvolysis of alkyl tosylates in rather poorly ionizing solvents such as acetic acid require a four-state reaction sequence (eq 2).

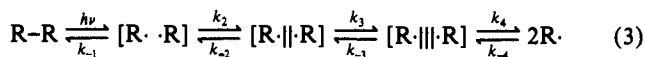


These species were viewed as singular stable species, and first-order rate constants were assigned to their interconversions.

Recently Kochi et al.⁹ found this kinetic description to be adequate for picosecond studies in which the rates of interconversion of these species were determined directly. Exponential relaxations were observed. Therefore the simplest form of diffusional theories do not seem to adequately describe these reactions involving complex ions. On the other hand, there is no doubt that the diffusive model describes geminate recombination of a proton to hydroxypyrenetrilsulfonate ion, as studied by Huppert, Pines, and Agmon.¹⁰ The long-range Coulomb force requires an ad-

ditional term in the Smoluchowski equation, but still a nonexponential, power law dependence was predicted and cleanly observed. We repeated the observation in our laboratory and could easily follow the recombination kinetics by fluorescence methods from 20 ps to 30 ns, at which time more than 99% of the geminate partners have recombined.¹¹

The second kind of reaction treated lies at the opposite extreme: the homolytic cleavage of iodine, disulfides, and azo compounds in nonpolar solvents. These are not expected to involve the strong solvation energies that ions display. In this case one might expect the diffusion theories to be applicable.



However this assumes that solvation energies of the various species do not differ greatly, and this has not been demonstrated in particular cases.

One might expect that the diatomic halogens, notably I₂, would meet the requirements for the application of the usual diffusive model; they should be good spherical reactive species. Even in that case, however, experimental measurables are dominated by details of vibrational cooling of pairs that separate slightly and recombine but never get far enough apart to be considered to be diffusing through solvent.¹² To our knowledge, power law kinetics have not yet been detected for I₂ recombination, even though there must be some small amount of such behavior on some time scale. On the other hand, recent studies of disulfides and azo compounds¹³ have shown kinetic behavior which is consistent with the Smoluchowski diffusion theory. For example, recovery after photolysis of azocumene with a 25-ps laser pulse was found to be nonexponential, and a square root of time dependence was observed.^{13a} In that case, insufficient time resolution prevented analysis of very early times when the assumptions of the diffusive model should not yet be valid.

The third class of geminate processes involves donor-acceptor complexes of metals.¹⁴



In this case, the polarity of the geminate partners is intermediate between that of ion pairs and that of hydrocarbon radical pairs. It is, therefore, unclear which description, continuous diffusion or the discrete species theory, would be the better first approximation. Indeed, the description might vary with the nature of the species undergoing photolysis. A number of picosecond kinetic studies¹⁵⁻²³ of heme proteins and iron porphyrin complexes with

(11) Magde, L. S.; Oakes, J.; Magde, D. Unpublished.

(12) (a) Chuang, T. J.; Hoffman, G. W.; Eiselthal, K. B. *Chem. Phys. Lett.* **1974**, *25*, 201. (b) Harris, A. L.; Brown, J. K.; Harris, C. B. *Annu. Rev. Phys. Chem.* **1988**, *39*, 341. (c) Xu, X.; Lingle, R.; Yu, S.-C.; Chang, Y. J.; Hopkins, J. B. *J. Chem. Phys.* **1990**, *92*, 2106.

(13) (a) Scott, T. W.; Liu, S. N. *J. Phys. Chem.* **1989**, *93*, 1393. (b) Scott, T. W.; Doubleday, C., Jr. *Chem. Phys. Lett.* **1991**, *178*, 9-18.

(14) (a) Scandola, F.; Scandola, M. A.; Bartocci, C. *J. Am. Chem. Soc.* **1975**, *97*, 4758. (b) Angermann, K.; Schmidt, R.; van Eldik, R.; Kelm, H.; Wasgestan, F. *Inorg. Chem.* **1982**, *21*, 1175.

(15) (a) Traylor, T. G.; Taube, D. J.; Jongeward, K. A.; Magde, D. *J. Am. Chem. Soc.* **1990**, *112*, 6875. (b) Taube, D. J.; Projahn, H. D.; van Eldik, R.; Magde, D.; Traylor, T. G. *J. Am. Chem. Soc.* **1990**, *112*, 6880. (c) Jongeward, K. A.; Magde, D.; Taube, D. J.; Traylor, T. G. *J. Biol. Chem.* **1988**, *263*, 6027. (d) Traylor, T. G.; Magde, D.; Taube, D.; Jongeward, K. A. *J. Am. Chem. Soc.* **1987**, *109*, 5864. (e) Traylor, T. G.; Magde, D.; Taube, D.; Jongeward, K. A.; Bandyopadhyay, D.; Luo, J.; Walda, K. N. *J. Am. Chem. Soc.* **1992**, *114*, 417. (f) White, D. K.; Cannon, J. B.; Traylor, T. G. *J. Am. Chem. Soc.* **1979**, *101*, 2443.

(16) Shank, C. V.; Greene, B. I. *J. Phys. Chem.* **1983**, *87*, 732.

(17) Noe, L. J.; Eisert, W. G.; Rentzepis, P. M. *Proc. Natl. Acad. Sci. U.S.A.* **1978**, *75*, 573.

(18) Greene, B. I.; Hochstrasser, R. M.; Weisman, R. B.; Eaton, W. A. *Proc. Natl. Acad. Sci. U.S.A.* **1978**, *75*, 5255.

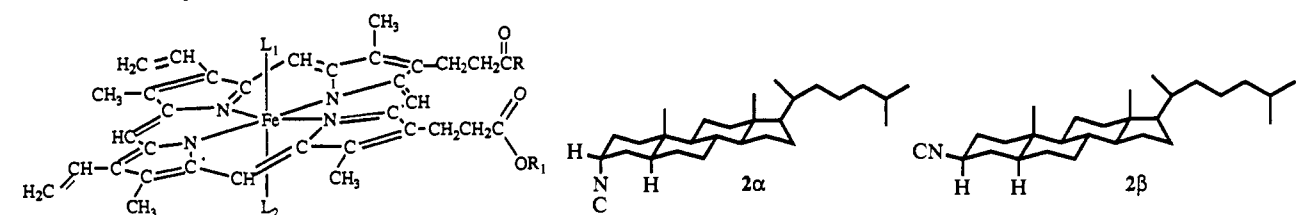
(19) Petrich, J. W.; Poyart, C.; Martin, J. L. *Biochemistry* **1988**, *27*, 4049.



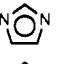
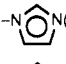
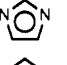
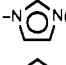
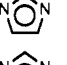
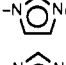
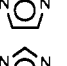
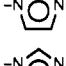



(20) Jongeward, K. A.; Magde, D. J.; Taube, D. J.; Marsters, J. C.; Traylor, T. G.; Sharma, V. S. *J. Am. Chem. Soc.* **1988**, *110*, 380.

(21) Jongeward, K. A.; Magde, D.; Taube, D. J.; Traylor, T. G. *J. Biol. Chem.* **1988**, *263*, 6027.

(9) (a) Masnovi, J. M.; Kochi, J. K. *J. Am. Chem. Soc.* **1985**, *107*, 7880. (b) Masnovi, J. M.; Kochi, J. K.; Hilinski, E. F.; Rentzepis, P. M. *J. Am. Chem. Soc.* **1986**, *108*, 1126. (c) Yabe, T.; Sankararaman, S.; Kochi, J. K. *J. Phys. Chem.* **1991**, *95*, 4177.

(10) (a) Pines, E.; Huppert, D.; Agmon, N. *J. Chem. Phys.* **1988**, *88*, 5620. (b) Huppert, D.; Pines, E.; Agmon, N. *J. Opt. Soc. Am. B.* **1990**, *7*, 1545.

Table I. Heme Complexes^a


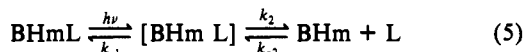
no.	solvent	heme	R	R ₁	L ₁	L ₂
1a	toluene	protoheme dimethyl ester	OMe	Me	2α	2α
1b	methylcyclohexane	protoheme dimethyl ester	OMe	Me	2β	2β
1c	toluene	protoheme dimethyl ester	OMe	Me	MeN 	MeN 
1d	toluene	protoheme dimethyl ester	OMe	Me	MeNC	MeNC
1e	benzene	monochelated protoheme methyl ester	NH(CH ₂) ₃ N 	Me	C ₆ F ₅ NC	-N  (chelated)
1f	toluene	monochelated protoheme methyl ester	NH(CH ₂) ₃ N 	Me	MeNC	-N  (chelated)
1g	benzene	monochelated protoheme methyl ester	NH(CH ₂) ₃ N 	Me	C ₆ Cl ₅ NC	-N  (chelated)
1h	methylcyclohexane	monochelated protoheme stearyl ester	NH(CH ₂) ₃ N 	stearyl	2α	-N  (chelated)
1i	toluene	monochelated protoheme stearyl ester	NH(CH ₂) ₃ N 	stearyl	tBuCH ₂ CM ₂ NC	-N  (chelated)
1j	glycerol/DMF	protoheme	OH	H	CO	MeN 

^aThe ligand L₁ dissociates upon photolysis as indicated in the difference spectra.¹⁵

O₂, NO, CO, isocyanides, imidazoles, etc. have been carried out with rather widely varying results and interpretations.

Frauenfelder et al.²² and Dlott and co-workers²³ have studied the rebinding of carbon monoxide after photolyses of heme protein-carbon monoxide complexes and simple heme-carbon monoxide complexes in low-temperature glasses and in high-viscosity solvents such as glycerol over wide temperature ranges. They report nonexponential kinetics for the concentration-independent processes and find relaxations extending over two or three powers of ten. Some results were interpreted in terms of the continuous diffusion model.

We have studied several geminate reactions in low-viscosity organic solvents. The photolyzed species was usually an imidazole-protoheme dimethyl ester-ligand complex from which the ligand was photolyzed with a 400-fs pulse.



We found only one concentration-independent relaxation, which was assigned to geminate recombination and fit to an exponential decay within the accuracy of our data. Of course, a concentration-dependent, bimolecular combination is also present at very long times. While there are differences in the two studies, ours involving faster reactions in lower viscosity solvents, such different kinetic observations on superficially similar reactions require an explanation. We considered the possibility that our earlier observations did not have sufficient signal to noise ratios to definitively establish the order of the reaction or might be compromised by subtle systematic distortions due to repeatedly photolyzing a relatively small volume of solution. We, therefore, re-

peated some of our earlier studies and examined other reactions with an improved apparatus in which the sample is circulated at a rate which replenishes the sample between individual pulses. Currently, data are collected every picosecond from 0 to 200 ps and at larger intervals to 8000 ps. This system allows us to describe the nature of the decay with greater confidence.

In this paper, we present several examples of the recombination of isocyanides, 1-methylimidazole, and carbon monoxide in simple systems such as chelated protoheme, protohemin, and heme proteins. Exponential decay is observed in every case. Our goal here is to establish a set of experimental data. If one must choose between limiting models, our data are better interpreted by the kinetic model.

Experimental Section

Materials. Dichloromethane and xylene were distilled over calcium hydride, and toluene was distilled over LiAlH₄ under nitrogen. Pentachloroaniline, pentafluoroaniline, triphosgene, triethylamine (99%), formic acid (96%), and xylene were purchased from Aldrich. Protohemin chloride (Calbiochem) and glycerol (Mallinckrodt) were used as purchased. Protohemin dimethyl ester, protohemin chloride, chelated protohemin chloride, and monostearyl ester chelated protohemin chloride were from previous studies.^{15d,24a,b} The preparations of 5α-cholestan-3α-yl isocyanide (2α) and 5α-cholestan-3β-yl isocyanide (2β) are described elsewhere.^{24a} The complexes photolyzed are listed in Table I.

Synthesis of Pentachlorophenyl Isocyanide (2,3,4,5,6-Pentachlorophenyl Isocyanide).²⁵ A mixture of 2,3,4,5,6-pentachloroaniline (1.0 g, 3.76 μmol), formic acid (30 mL, 0.8 mol), and xylene (30 mL) was refluxed for 3 days. After the removal of the volatiles by heating under vacuum, a 1/1 mixture of (pentachlorophenyl)formamide and starting material was obtained. The above mixture (480 mg) was dissolved in methylene chloride (30 mL); then triethylamine (0.8 mL) was added. Methylene chloride (10 mL) containing triphosgene (400 mg, 1.35 mmol) was added dropwise to the above solution with stirring in an ice-water bath over a period of 20 min. The resulting solution was stirred for

(22) (a) Alberding, N.; Austin, R. H.; Chan, S. S.; Eisenstein, L.; Frauenfelder, H.; Good, D.; Kaufman, K.; Marden, M.; Nordlund, T. M.; Reinisch, L.; Reynolds, A. H.; Sorensen, L. B.; Wagner, G. C.; Yue, K. T. *Biophys. J.* **1978**, *24*, 319. (b) Ansari, A.; Dilorio, E. E.; Dlott, D. D.; Frauenfelder, H.; Iben, I. E. T.; Langer, P.; Roder, H.; Sauke, T. B.; Shyamsunder, E. *Biochemistry* **1986**, *25*, 3139.

(23) (a) Postlewaite, J. C.; Miers, J. B.; Dlott, D. D. *J. Am. Chem. Soc.* **1989**, *111*, 1248. (b) Miers, J. B.; Postlewaite, J. C.; Cowen, B. R.; Roemig, G. R.; Lee, I.-Y. S.; Dlott, D. D. *J. Chem. Phys.* **1991**, *94*, 1825. (c) Miers, J. B.; Postlewaite, J. C.; Zyung, T.; Chen, S.; Roemig, G. R.; Wen, X.; Dlott, D. D.; Szabo, A. J. *J. Chem. Phys.* **1990**, *93*, 8771.

(24) (a) Traylor, T. G.; Magde, D.; Taube, D. J.; Luo, J.; Walda, K. N. *J. Am. Chem. Soc.* Submitted. (b) Taube, D. C.; Traylor, T. G.; Magde, D.; Walda, K. N.; Luo, J. *J. Am. Chem. Soc.*, in press. (c) Traylor, T. G.; Magde, D.; Luo, J.; Walda, K. N. *J. Am. Chem. Soc.*, in press. (d) Sharma, V. S.; Magde, D.; Traylor, T. G.; Bandyopadhyay, D. *Biochem. J.* Submitted. (25) Ugi, I.; Fetzer, U.; Eholzer, U.; Knupfer, H.; Offermann, K. *Angew. Chem., Int. Ed. Engl.* **1965**, *4*, 472.

another hour at room temperature and then washed with water. The organic solvent was removed by rotary evaporation, the residue was purified on a Chromatotron (silica gel, 3/1 cyclohexane/benzene), and pentachlorophenyl isocyanide was obtained (102 mg, 20%). Mp 161–163 °C; IR (CCl₄) 2110 cm⁻¹ (s).

Pentafluorophenyl isocyanide (2,3,4,5,6-pentafluorophenyl isocyanide) was prepared similarly. IR (CH₂Cl₂) 2125 cm⁻¹.

Kinetic Methods. Solutions of the heme complexes **1a–1j** were prepared by dissolving the hemin chloride in the solvent (~2 mL) in a test tube sealed with a serum cap and purging with nitrogen for 1–2 h. Ligands were added from standard, degassed solutions at this point if they were solid or after dilution if they were liquids. The hemin solution was reduced by adding 3 μL of a saturated methanol solution of sodium dithionite–18-crown-6 and stirring and diluted with degassed solvent to bring the Soret band absorbance to ~1.5 in a 2-mm cell. This tube was connected to a closed recirculating system consisting of a length of tygon tubing having a 2-mm-square quartz tubing in line and stainless steel needles at either end by inserting the two needles into the test tube. The system was purged with the appropriate gas before assembly. The solution was circulated at a rate (2–6 mL/min) which replenished the sample between each laser pulse (10-Hz frequency) using a peristaltic pump. The sample **1j** in glycerol/DMF was prepared as previously described^{15c} except that dimethylformamide was added.

The picosecond (0.4-ps pulse width) photolyses were carried out with the ring laser system¹⁹ previously described²⁰ and the data accumulated as a series of spectra in 1-ps intervals up to 200-ps and 1-ns intervals up to 8 ns. These data were displayed as series of difference spectra^{15a,e} (pumped–unpumped), as absorbance versus time at one wavelength, or as single-value decomposition decays (absorbance versus time). Typical difference spectra have been published.^{15a,d}

Results and Discussion

We have chosen the photolyses of heme–isocyanide complexes as our principal study for several reasons. The quantum yields for photolysis to separate species²⁶ are commensurate with our observation of around 50% picosecond return, which offers strong evidence that the picosecond kinetic studies are monitoring geminate recombination. The concentrations can be varied from very low to pure isocyanide solvent, affording an opportunity to observe the competition between geminate recombination and scavenging by solvent. Thirdly, the size of the isocyanide can be varied and any effect upon cage processes observed.

Let us first consider the predictions of the kinetic model.



Throughout this study, concentrations were adjusted so that $k_{-2}[\text{BHm}][\text{RNC}]$ was orders of magnitude less than k_{-1} and k_2 . The photodissociation process represented by $h\nu$ was an impulsive “delta function.” (In fact, we had the time resolution to investigate electronic and vibrational relaxation that might be involved in forming [BHm CNR]; but that is not of interest here.) Under these conditions, the disappearance of [BHm CNR] obeys simple first-order decay with exponential rate constant $k_{\text{obs}} = k_{-1} + k_2$ to a “plateau” which revealed the photodissociation yield Φ given by $\Phi = k_2/(k_{-1} + k_2)$.

It is instructive to consider a case for which $k_{-1} \gg k_2$. Then $k_{\text{obs}} = k_{-1}$ and $\Phi = 0$. Such a case was examined in a previous study of iron(II) cytochrome *c* and iron(II) cytochrome *b₅*.²¹ Examination of the X-ray crystal structure of cytochrome *c* reveals that there is just enough space to allow the iron–imidazole bond to break by rotation around C–C bonds, but no more. There is no solvent, no diffusion, and no protein movement on the picosecond time scale. The barrier represented by k_2 is effectively infinite. The barrier represented by k_{-1} involves bond rotation and nonbonded interactions with neighboring amino acids. Therefore, this is a true return from the contact pair without diffusion. It was expected and found to be an exponential process.

For this study, we first designed geminate partners for which k_2 might be small, namely very large isocyanides. We show in Figure 1 the absorbance change versus time after photolysis of the protoheme dimethyl ester–bis(5 α -cholestan-3 α -yl isocyanide)

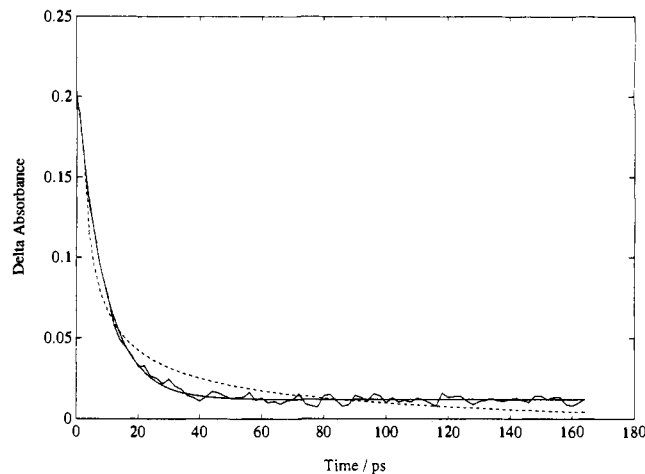


Figure 1. Kinetic trace for picosecond transient absorption in PHDME(5 α -cholestan-3 α -yl isocyanide)₂ (**1a**) in toluene. [Heme] = 1×10^{-5} M; [5 α -cholestan-3 α -yl isocyanide] = 8×10^{-4} M. The change in absorbance at 433 nm is plotted vs time delay between the pump and the probe pulses. The smooth solid line is an exponential fit which reveals a rate constant of 1.1×10^{11} s⁻¹ and a return of 95%. The dashed line is the best fit to a diffusive model, as described in the text.

complex in toluene. This plot reveals 95% return ($\Phi = 0.05$) to starting state in less than 40 ps. The bond-making process k_{-1} dominates the kinetics. Therefore, we again expect and find accurate exponential decay. We show the data to about 27 half-lives, and we can observe the remaining 5% return on a very slow time scale commensurate with its bimolecular rate constant. There is no significant “missing amplitude” that might be recombining at intermediate times.

The data in Figure 1 are also tested against the predictions of the diffusive model, solved in the usual manner for interacting spheres confined to a half-space,^{23c} as might be expected for ligand binding to porphyrins. The transient absorbance change, proportional to the survival probability of [BHm CNR], is given by a simple expression, if a certain approximation is valid:^{23c}

$$\Delta A \propto (1 - \Phi) \exp(\tau) \text{erfc}(\tau^{1/2}) \quad (7)$$

where erfc is the complementary error function and $\tau = Dt/R^2\Phi^2$. Furthermore, D is the relative diffusion constant, equal to the sum of the translational diffusion constants of the two geminate partners, t is time, and R is the reaction distance, equal to the sum of the radii of the reaction partners for hard spheres. The chemistry is hidden in $\Phi = k_D/(k_0 + k_D)$, where $k_D = 2\pi DR$, for the half-space geometry, and k_0 has the units of a bimolecular rate constant and is a measure of the intrinsic rate of reaction at contact. If reaction occurs in every encounter, $k_0 \rightarrow \infty$; if no reaction ever occurs, $k_0 \rightarrow 0$.

The required condition for a more complicated expression to simplify to eq 7 is $D/R^2\Phi^2k_0C \gg 1$. For order-of-magnitude estimates, we take $D = 10^{-6}$ cm² s⁻¹, $R = 10^{-7}$ cm, $\Phi = 0.05$, and $C = 1$ mM = 10^{18} cm⁻³. Then the inequality requires $k_0 \ll 10^{-6}$ cm³ s⁻¹, which is $k_0 \ll 10^{15}$ L mol⁻¹ s⁻¹. For the same D and R , the order of magnitude of $k_D = 10^{-12}$ cm³ s⁻¹. Using the expression for Φ , we can estimate $k_0 = 10^{-11}$ cm³ s⁻¹ = 10^{10} M⁻¹ s⁻¹, approximately; so the condition is easily satisfied.

An independent determination of k_0 is available from a measurement of the bimolecular combination rate constant $k_{\text{on}} = k_D(1 - \Phi)$. We determined $k_{\text{on}} = (6.1 \pm 0.5) \times 10^7$ M⁻¹ s⁻¹ for the system in Figure 1. This is 100 times smaller than predicted by the discussion above. The discrepancy cannot be eliminated entirely by revising the values for D and R . Rather, one must argue that there is a significant geometric factor for those reactants compared to spheres.

The dashed line in Figure 1 is the best fit of the data to the diffusive model, eq 7. The fit is poor. In addition, values for the fitting parameters are unrealistic. The y -intercept, $\Delta A(\tau=0)$, should be near 0.2; but the dashed line actually rises to 1600, which

(26) Olson, J. S.; McKinnie, R. E.; Mims, M. P.; White, D. K. *J. Am. Chem. Soc.* **1983**, *105*, 1522.

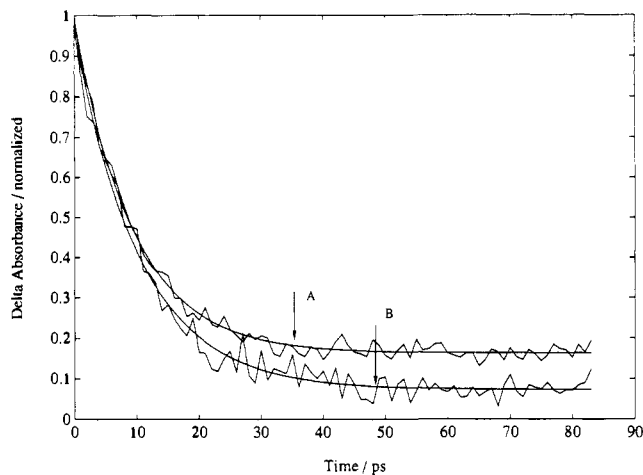


Figure 2. (A) Kinetic trace for picosecond transient absorption in PHDME(5α -cholestan- 3β -yl isocyanide) $_2$ (**1b**) in methycyclohexane. $[\text{Heme}] = 1 \times 10^{-5} \text{ M}$; $[5\alpha\text{-cholestan-}3\beta\text{-yl isocyanide}] = 1.5 \times 10^{-3} \text{ M}$. The change in absorbance at 430 nm is plotted vs time delay between the pump and the probe pulses. The exponential fit, shown as a smooth line, gives the overall rate constant of $1.2 \times 10^{11} \text{ s}^{-1}$ with 84% return. (B) Kinetic trace for the dominant component of a singular value decomposition analysis of protoheme PHDME(1-methylimidazole) $_2$ (**1c**) in toluene after picosecond laser photolysis. $[\text{Heme}] = 1 \times 10^{-5} \text{ M}$; $[1\text{-methylimidazole}] = 3 \times 10^{-3} \text{ M}$. The absorbance change at all times is plotted vs time delay between the pump and the probe pulses. Ninety-one percent recovery of the spectrum at all wavelengths with a first-order rate constant of $1.0 \times 10^{11} \text{ s}^{-1}$ was observed.

cannot be plotted. The asymptotic value of ΔA at long times is -0.017 , even though negative values are unphysical. Hence, $\Phi = -0.017/1600 = -1 \times 10^{-5}$, in contradiction to the known value near 0.05. The scale factor for the dimensionless reduced time τ is $D/R^2\Phi^2 = 1.16 \times 10^{13} \text{ s}^{-1}$.

We can constrain any one fitting parameter to a reasonable value. In particular, we can force Φ to be positive. That does not help; it just leads to even less plausible values for the other parameters.

Figure 2A shows a similar plot using the β isomer of this isocyanide, 5α -cholestan- 3β -yl isocyanide, in which 84% return is observed. Again, an exponential decay is observed and the absorbance reaches a steady value in less than 40 ps. The absorbance remains constant until a bimolecular return begins, a time which depends upon concentration of ligands and can be as long as one ms. These observations are confirmed by the very low photodissociation quantum yields and consequent difficulties in observing the bimolecular processes on slower time scales. Similar kinetics were observed in different solvents.

Exponential rebinding is not confined to very large isocyanides. As another example with large k_{-1} and small k_2 , we considered 1-methylimidazole. The kinetics of absorbance change after picosecond photolysis of protoheme dimethyl ester bis(1-methylimidazole) (**1c**), shown in Figure 2B, is also exponential. Again, since the return is about 90%, k_2 contributes little to k_{obs} .

Figure 3 shows the exponential excited-state decay after photolysis of PHDME(MeNC) $_2$ in toluene. There is no rebinding of ligand to the five-coordinated heme during this relaxation process. Again, exponential decay is expected and is observed. Excited-state decay will be discussed elsewhere.^{24b} The point to be made is that geminate return shows the same exponential behavior as does excited-state relaxation, a known first-order process.

Although both the kinetic model and the diffusion model can describe any value of Φ , that is any ratio of k_{-1}/k_2 , one might suspect that the diffusion description would be more evident for $k_{-1}/k_2 = 1$. We next investigate smaller isocyanides in which $k_2 \approx k_{-1}$. Figure 4 shows three return curves after photolyses of chelated protoheme complexes of pentafluorophenyl isocyanide (A), of methyl isocyanide (B), and of 5α -cholestan- 3α -yl isocyanide (C). Although different quantum yields (returns of 49,

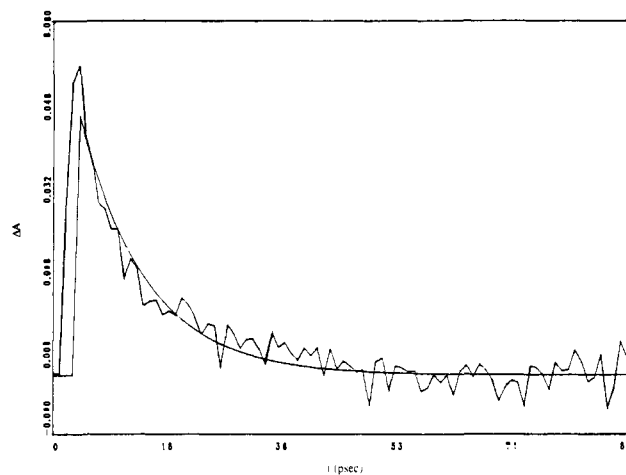


Figure 3. Kinetic plot for the excited-state decay of PHDME(MeNC) $_2$ (**1d**) in toluene. $[\text{Heme}] = 1 \times 10^{-5} \text{ M}$; $[\text{MeNC}] = 4.9 \times 10^{-3} \text{ M}$. The absorbance change at 444 nm is plotted vs time delay between the pump and the probe pulses. The first-order kinetic fit shown gives a rate constant of $9.7 \times 10^{10} \text{ s}^{-1}$.

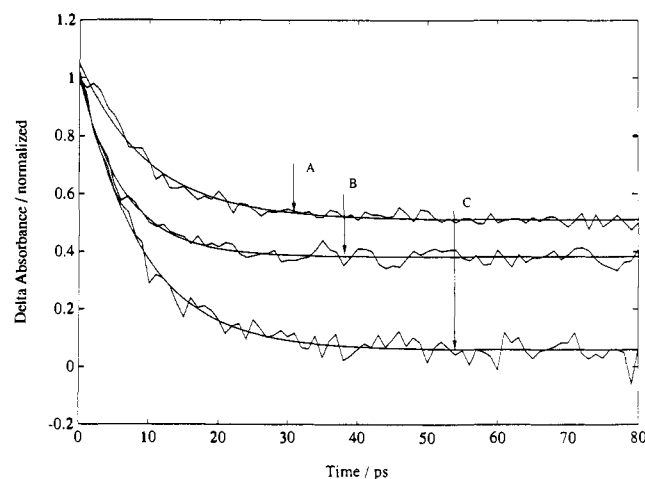


Figure 4. (A) Singular value decomposition decay plot of monochelated protoheme-pentafluorophenyl isocyanide (**1e**) in benzene. $[\text{Heme}] = 1 \times 10^{-5} \text{ M}$; $[\text{F}_5\text{C}_6\text{NC}] = 4.9 \times 10^{-3} \text{ M}$ ($\lambda_{\text{max}} 425 \text{ nm}$). The absorbance change at all wavelengths is plotted vs time delay between the pump and the probe pulses. A 49% return of the spectrum at all wavelengths with a rate constant of $1.2 \times 10^{11} \text{ s}^{-1}$ was observed. (B) Kinetic plot of monochelated protoheme-methyl isocyanide **1f** in toluene. $[\text{Heme}] = 1 \times 10^{-5} \text{ M}$; $[\text{MeNC}] = 7.4 \times 10^{-3} \text{ M}$. The absorbance change at 428 nm is plotted vs time delay between the pump and the probe pulses. The first-order kinetic fit shown gives a rate constant of $1.4 \times 10^{11} \text{ s}^{-1}$ and 54% return of the six-coordinated species. (C) Picosecond transient absorption decay for monostearyl ester chelated protoheme- 5α -cholestan- 3α -yl isocyanide **1h** in toluene. $[\text{Heme}] = 1 \times 10^{-5} \text{ M}$; $[5\alpha\text{-cholestan-}3\alpha\text{-yl isocyanide}] = 1 \times 10^{-3} \text{ M}$. The change in absorbance at 428 nm is plotted as a function of time delay between the pump and the probe pulses. A 95% recovery of the six-coordinated species with the observed rate constant of $9.7 \times 10^{10} \text{ s}^{-1}$ is observed.

54, and 95%) were obtained, all three traces display exponential decay. Another case of such a process treated in more detail is shown in Figure 5, where geminate recombination of the monochelated protoheme-pentachlorophenyl isocyanide complex is characterized. In this case, there is 64% return and 36% escape and the decay is accurately exponential. The absorbance becomes constant in 60 ps with a first-order rate constant of 10^{11} s^{-1} and remains unchanged to the end of the measurements, which was 200 ps. In separate experiments, we have extended the time to 8000 ps and observed no further change in absorbance. Therefore, certainly the great majority and probably all of the geminate recombination in this isocyanide reaction is completed in less than 50 ps. Also shown in Figure 5 is the best fit to the diffusive model, eq 7. The fit is quite unsatisfactory, and again as in Figure 1,

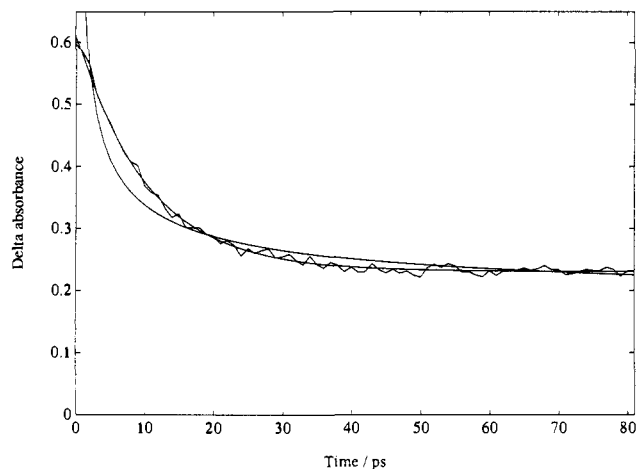


Figure 5. Singular value decomposition decay plot of monochelated protoheme-pentachlorophenyl isocyanide **1g** in benzene. [Heme] = 1×10^{-5} M; [Cl₅C₆NC] = 4.9×10^{-3} M (λ_{max} 425 nm). The absorbance change at all wavelengths is plotted vs time delay between the pump and the probe pulses. A 64% return of the six-coordinated species with a rate constant of 9.7×10^{10} s⁻¹ was observed. See text.

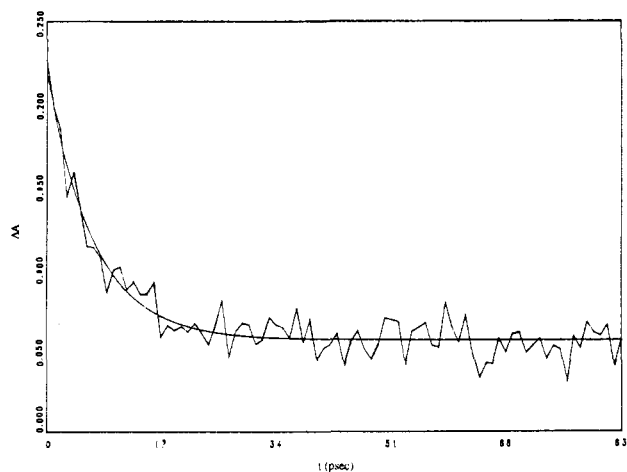


Figure 6. Picosecond transient for monostearyl ester chelated protoheme-1,1,3,3-tetramethylbutyl isocyanide **1i** in toluene. [Heme] = 1×10^{-5} M; [1,1,3,3-tetramethylbutyl isocyanide] = 4×10^{-4} M. The change in absorbance at 428 nm is plotted as a function of time delay between the pump and the probe pulses. A 75% return of the six-coordinated species with the observed rate constant of 1.4×10^{11} s⁻¹ was observed.

the fitting parameters are unrealistic. The $\Delta A(\tau=0) = 16\,500$ instead of 0.7; the asymptote is 0.164, which is too small; and $D/R^2\Phi^2 = 2.86 \times 10^{14}$. Figure 6 displays the return after photolysis of an isocyanide of intermediate size (1,1,3,3-tetramethylbutyl isocyanide). As might be expected, more return is observed (75%) than that in the case of methyl isocyanide (54%). The relaxation is again accurately exponential. The photolysis of the horseradish peroxidase (Fe²⁺) complex of methyl isocyanide showed picosecond delay which was as accurately exponential as any of the plots shown.

Having found no evidence for diffusive recombination in any of the isocyanides, we reexamined the behavior of carbon monoxide. Since CO shows no measurable geminate recombination in low-viscosity solvents, we photolyzed the complex 1-methylimidazole-protoheme dimethyl ester-carbon monoxide in a solvent mixture of 5% dimethylformamide in glycerol at 25 °C. The DMF is added to improve solubility and prevent aggregation. The species being photolyzed is unequivocally 1-methylimidazole-protoheme dimethyl ester-carbon monoxide.^{15c} Picosecond photolysis reveals no extra recombination at early picosecond times, just the initial linear portion of a concentration-independent geminate recombination that continues over hundreds of picoseconds—a situation quite different from any of the cases considered above. Figure

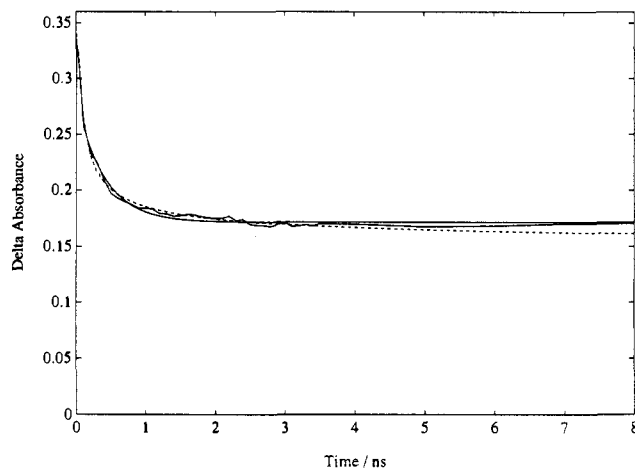


Figure 7. Transient decay at 420 nm and fits for recombination of CO in protoheme-carbon monoxide **1j** in 1% 1-methylimidazole/5% DMF/94% glycerol: solid line, single exponential fit; dashed line, diffusion fit.

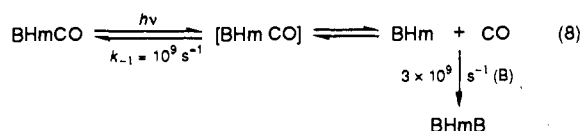
7 shows the kinetics of transient absorption changes along with theoretical fits to the kinetic model and the diffusion model. The exponential fit requires a rate constant $k_{\text{obs}} = 2.6 \times 10^9$ s⁻¹ and $\Phi = 0.61$, with the asymptote reached within 1 ns and no further recombination until bimolecular combination begins at much longer times. The exponential fit would be considered acceptable for some purposes, but it is not perfect. Of course, if one hypothesizes multiple solvation states and fits to two exponentials, using four free parameters, the fit can be made essentially perfect. A fit to the diffusion model is also shown. It uses the parameters $\Delta A(\tau=0) = 1.4$, asymptote = 0.15, and $D/R^2\Phi^2 = 3.5 \times 10^{11}$ s⁻¹. Over the time range 0.1–3.6 ns, where most of the geminate recombination is occurring, the fit is slightly superior to the single exponential; a χ^2 test shows a (barely) significant difference. However, outside that region, the diffusion fit is not so successful. The $t = 0$ intercept is patently incorrect. However, the diffusion model should not be expected to apply at very early times. Earlier work^{23c} that found evidence for diffusive recombination did not have adequate time resolution to explore this region. There is also a discrepancy at long times. The power law decay of the diffusive fit approaches its asymptotic value very slowly. Between 4 and 8 ns it is already beginning to fall below the data, and it continues to decrease slowly. Unfortunately, it is difficult to be certain that there are no systematic errors of that small magnitude in our data at long times. If we use the fitted asymptote with the known $\Delta A(\tau=0)$, rather than the unrealistic fitted value, we find $\Phi = 0.52$ in this model. There is some similarity between this work and the earlier study. In both cases, the experimental data actually fall between the theoretical curves for the competing models. The earlier study used a smaller fraction of glycerol, which implies a lower viscosity and a larger Φ , as was observed. However, our value for $D/R^2\Phi^2$ is almost 100 times larger, which is not easily explained.

Diffusion Model vs Kinetic Model. The diffusion model is fundamental in the following sense: Once the bimolecular recombination rate constant is measured, assuming that diffusion constants and molecular radii are known or estimated, it must fit the complete time course of geminate recombination with no adjustable parameters. Such a theory merits attention, even if it is not perfect; and the diffusion model, as solved up until now, is not expected to be complete in as much as it treats the solvent as a continuum at all times, even very early times, and treats the reaction partners as simple spheres, ignoring all geometric detail. The kinetic model has two completely arbitrary parameters, k_{-1} and k_2 , and can always fit a restricted time range. The models may be distinguished by sufficiently precise measurements over sufficiently complete time ranges. Neither this study of CO binding nor the previous one^{23c} is entirely adequate. The best argument is that the previous study was able to fit not only room temperature data but data for a wide range of temperatures with

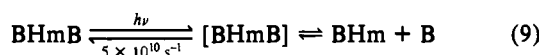
a single consistent set of parameters. We suspect that a complete description will, in some sense, be intermediate between the limiting models. However, our goal here is not to refine the analysis of CO recombination. Our principal goal is to demonstrate that we would be able to recognize diffusive recombination if it should occur and, thereby, strengthen the conclusion that none of the isocyanides can be described by the diffusion limit.

Mechanisms of Isocyanide-Heme Reactions. We have shown that geminate processes which occur after photolyses of an isocyanide from an imidazole-heme-isocyanide complex are accurately described by a single exponential with a first-order rate constant around 10^{11} s^{-1} . This was true whether $k_{-1} \approx k_2$ or they were somewhat different. We therefore conclude that both combination (k_{-1}) and separation (k_2) are first-order processes. The fact that the absorbance becomes constant after a few half-lives argues strongly against the power law behavior, and the fact that k_{obs} is as fast as it is makes it impossible to find any reasonable parameters for the diffusion model.

We previously showed that when 1-methylimidazole-protoheme dimethyl ester-carbon monoxide is photolyzed in toluene, no picosecond return is observed, whereas, in 1-methylimidazole as solvent, return of 1-methylimidazole was observed.^{24c}

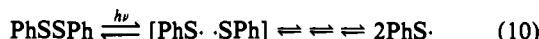


The fact that 1-methylimidazole reacts from solvent at a rate which is consistent with the bimolecular rate constant times its concentration ($2 \times 10^8 \text{ M}^{-1} \text{ s}^{-1}$)^{24c} and about 10 times slower than geminate return of the same base (eq 9) makes it clear that



geminate processes are finished by the time this process begins. The ligand becomes randomly distributed with the solvent in <100 ps.

It is interesting to contrast our results for the geminate behavior of the [BHm L] pairs with that of phenylthiyl radical pairs reported by Scott and Liu.^{13a} In both cases, low- to medium-viscosity hydrocarbon solvents have been used, and in both cases, rather similar rates of the geminate reactions were observed (e.g., the first half-life is about 10 ps in both types of reactions). In our studies, where L = isocyanides or imidazoles, the geminate decay is clearly exponential and no further change in absorption occurs after ~40 ps. However, the photolysis of diphenyl disulfide in liquid decalin results in a decay curve with a first half-life of 21 ps, but the absorbance change from 100 to 1000 ps is at least half of that which occurs in the first 100 ps. The continuum diffusion model accurately describes this decay.

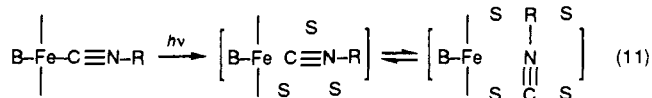


By contrast, no detectable change occurs in the [BHm L] system after ~5 half-lives (50 ps). Therefore, there is a fundamental difference in these two types of reactions, reactions 5 and 10.

These differences indicate that there are geminate processes which do not follow the continuum diffusion model, i.e., in which some other phenomenon dominates the kinetic behavior. The BHm + L systems where L = imidazoles and isocyanides are such systems. It is not yet clear whether this is the case with the other ligands such as L = CO although our results seem to suggest that neither extreme model applies precisely at all times.

We must therefore look for some chemical phenomenon which would convert the continuum diffusion system to a simple first-order decay. The solvation of the contact pair, causing it to be stabilized toward rebinding or dissociation, would have the effect of presenting the appropriate barriers to produce kinetic, i.e., first-order decay. Because the ligands are somewhat polar, it is

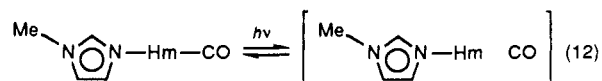
possible that some special stabilization develops for the contact pair, perhaps involving an orientation of the ligand resembling the bound state (S = solvent molecule).



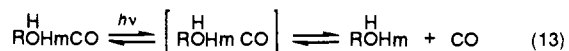
In this scheme, the increased solvation and reorientation would both inhibit recombination.

If the contact pair separation is largely a rotation process, then we should expect isocyanides bound within heme proteins to be similar to simple hemes in solution with regard to picosecond kinetics. We previously reported that the picosecond relaxations after photolyses of myoglobin isocyanides and chelated protoheme isocyanides are very similar.^{15d,20} The isocyanides are sufficiently large to fill the heme pocket. The larger ones distort the pocket. They may be limited to rotational motion, although protein conformational changes can affect the motion. Neither the protein nor the model system shows power law behavior in the fast geminate recombination of isocyanides. This suggests that proteins are accurately modeled with heme complexes in low-viscosity solvents for isocyanide binding. Small diatomic ligands could demonstrate additional features. Previous studies indicate that ion pair geminate reactions show progressions through discrete intermediates in first-order processes⁹ whereas combination of thiyl radicals^{13a} or of cumyl radicals^{13b} is best described in terms of the continuous diffusion model. The present results suggest that heme plus ligand recombinations involve a single discrete intermediate (contact pair) which disappears in a first-order process for ligands such as isocyanides or imidazoles. Neither the solvent-separated pair, such as that seen in ionic reaction, nor the nonexponential diffusion, expected from diffusion theory, are observed.

It is not clear why our observation of CO return differs from those previously reported.^{23a} We photolyze a single, well characterized species (eq 12), and we have shown that photolysis



produces a single five-coordinated species which cannot add 1-methylimidazole at this low concentration (eq 12).^{15b} Thus, we are observing a single recombination process. In the absence of 1-methylimidazole, the heme-carbon monoxide complex adds solvent, producing a mixture of primary and secondary glycerol complexes and the aquo complex (eq 13).^{15c} It is therefore possible



that more than one caged species was obtained. Alternatively, small errors in absorbance measurements in either study could cause such differences. A direct comparison of the two systems will help to resolve these discrepancies.

The results presented here provide strong evidence that the photolysis of model compounds for heme proteins in which the photolyzed compound is an imidazole-heme-ligand complex results in an exponential decay of the photolyzed (cage) product in which 49 to 95% return to the starting compound is observed. This behavior was observed for isocyanides and 1-methylimidazole. For CO, where geminate recombination is observed only at high viscosity, the situation is not yet clear. These data are interpreted as recombination from a contact pair in competition with rotation and solvation.

Acknowledgment. We are grateful to the National Institutes of Health (Grant HL 13581) and to the National Science Foundation (Grants CHE-8715561 and CHE-9114613) for support.